

# Classification Using Functional Data Analysis for Temporal Gene Expression Data

Xiaoyan Leng<sup>a\*</sup>, Hans-Georg Müller<sup>b</sup>

<sup>a</sup>Wake Forest University School of Medicine, Public Health Sciences, Section on Biostatistics, Medical Center Blvd., MRI-3, Winston-Salem, NC 27157, <sup>b</sup>Department of Statistics, University of California, One Shields Avenue, Davis, CA 95616

## ABSTRACT

**Motivation:** Temporal gene expression profiles provide an important characterization of gene function, as biological systems are predominantly developmental and dynamic. We propose a method of classifying collections of temporal gene expression curves in which individual expression profiles are modeled as independent realizations of a stochastic process. The method uses a recently developed functional logistic regression tool based on functional principal components, aimed at classifying gene expression curves into known gene groups. The number of eigenfunctions in the classifier can be chosen by leave-one-out cross-validation with the aim of minimizing the classification error.

**Results:** We demonstrate that this methodology provides low-error-rate classification for both yeast cell cycle gene expression profiles and *Dictyostelium* cell-type specific gene expression patterns. It also works well in simulations. We compare our functional principal components approach with a B-spline implementation of functional discriminant analysis for the yeast cell cycle data and simulations. This indicates comparative advantages of our approach which uses fewer eigenfunctions/base functions. The proposed methodology is promising for the analysis of temporal gene expression data and beyond.

**Availability:** MATLAB programs are available upon request.

**Contact:** lieng@wfubmc.edu

**Supplementary Information:** Supplementary Materials are available on the journal's web site.

## 1 INTRODUCTION

Since cDNA and oligonucleotide microarray techniques were developed to monitor the expression of many genes in parallel (Schena *et al.*, 1995; Schena *et al.*, 1996), this high-capacity system has been applied routinely for identifying and analyzing genes involved in various biological processes in different organisms (Spellman *et al.*, 1998; Cho *et al.*, 1998; Eisen *et al.*, 1998; Wen *et al.*, 1998; Golub *et al.*, 1999; Iyer *et al.*, 1999; White *et al.*, 1999; Hill *et al.*, 2000; Laub *et al.*, 2000; Cho *et al.*, 2001; Iranfar *et al.*, 2001; Breyne and Zabeau, 2001). Recently, microarray experiments are widely used to collect large-scale temporal data to monitor gene expression underlying development or other dynamic processes in many organisms. For example, a precise regulation of gene activity likely controls the molecular processes of DNA replication, chromosome segregation and mitosis during the cell cycle, which makes the study of

cell cycle dependent genome-wide expression an attractive system for genetic analysis. The first genome-wide expression analyses of cell cycle regulating genes were performed in budding yeast by Spellman *et al.* (1998). More recently, several other genome-wide expression studies of cell cycle regulated genes have been completed in bacteria (Laub *et al.*, 2000), fission yeast (Rustici *et al.*, 2004; Peng *et al.*, 2005), plants (Breyne *et al.*, 2001) and humans (Cho *et al.*, 2001).

Another widely studied organism is the amoeba, *Dictyostelium discoideum*, which provides opportunities for studying fundamental cellular processes, including aspects of development such as cell-type determination. Recent work on *Dictyostelium* includes a review by Mohanty and Firtel (1999) on mechanisms controlling spatial patterning and cell-type proportioning, and a study of gene expression patterns with microarrays by Shaulsky and Loomis (2002). Cell-type specific gene expression patterns were studied in *Dictyostelium* by Iranfar *et al.* (2001). Other types of gene expression data were generated in large-scale temporal gene expression studies in the mapping of development of the mouse central nervous system (Wen *et al.*, 1998), physiological response of human fibroblasts to serum (Iyer *et al.*, 1999), and development of *C. elegans* (Hill *et al.*) and *Drosophila* (White *et al.*, 1999; Arbeitman *et al.*, 2002). Information gleaned from the analysis of temporal gene expression profiles will provide an added dimension to insights into the characterization and of gene function.

For these large-scale data, classifying genes into different functional groups is a first step in order to gain more sophisticated knowledge of different biological pathways and/or functions. Many classification analyses have been performed for such temporal gene expression profiles. Hierarchical clustering (Spellman *et al.*, 1998; Eisen *et al.*, 1998; Wen *et al.*; Iyer *et al.*, 1999, Gasch *et al.*, 2000; Qin *et al.*, 2003), *k*-means clustering (Tavazoie *et al.*, 1999; Wu *et al.*, 2003), principal component analysis (PCA) and singular value decomposition (SVD) (Alter *et al.*, 2000, 2003; Raychaudhuri *et al.*, 2000; Li *et al.*, 2002; Holter *et al.*, 2000), self-organizing maps or its variants (Tamayo, *et al.*, 1999; Nikkila, *et al.*, 2002; Resson *et al.*, 2003), correlation analysis (Kruglyak and Tang, 2001) and independent component analysis (ICA) (Liebermeister, 2002; Lee and Batzoglou, 2003), as well as simulated annealing (Lukashin and Fuchs, 2001), and support vector machines (SVM) (Brown *et al.*, 2000) have been used.

These statistical and computational methods belong to the general framework of multivariate analysis, that is, data are treated as vectors of discrete samples and permutation of components will not

\*to whom correspondence should be addressed

affect the analysis results, hence the timing of the biological processes is irrelevant in these analyses. A more efficient way to look at such data is to incorporate the information that is inherent in time order and smoothness of processes over time. The tools for such an approach are provided by the recently developed methodology of functional data analysis (FDA, Ramsay and Silverman, 2005), especially discrimination and classification methods based on FDA (Hall *et al.*, 2001; James and Hastie, 2001; Müller, 2005), dynamic time warping (Aach and Church, 2001; Liu and Müller, 2003), and periodicity analysis (Zhao *et al.*, 2004). Recent non-parametric applications for the analysis of temporal gene expression data include work by Klevecz and Murray (2001), Luan and Li (2003), and Bar-Joseph *et al.* (2003). In the latter two papers, B-spline approaches to cluster genes based on mixed effects and mixture models were emphasized.

We view the observed gene expression profiles as independent realizations of a smooth stochastic process. The covariance function of the process is then also smooth and can be expanded into smooth orthogonal eigenfunctions (functional principal components), leading to the *Karhunen–Loève* representation of the observed sample paths as a sum of a smooth mean trend and an expansion of the random part in terms of these eigenfunctions. A truncated version of the random part of this representation serves as a statistical approximation of the random process (Rice and Silverman, 1991). In this paper, we consider functional discrimination through logistic regression based on functional principal components. We demonstrate the usefulness of this approach in a simulation study and for the analysis of yeast cell cycle temporal data, as well as for data on the differential expression patterns of *Dictyostelium* cell-type specific genes. Although our methods do not require a regular time design, these two data sets happen to have equally spaced time points. For more details on FPCA methods for irregular and/or sparse data, see Yao *et al.* (2005).

An alternative way to model random curves is provided by B-splines, which have been previously used for clustering problems. Rice and Wu (2001) proposed a non-parametric mixed effect model based on B-splines, see also Shi *et al.* (1996) and Luan and Li (2003), who emphasized cluster analysis derived from these approaches. We compared our approach based on functional principal components with a B-spline implementation of functional discriminant analysis for the yeast cell cycle data and in a simulation study. This indicates comparative advantages of our approach, which unlike the B-spline based model does not rely on Gaussian assumptions.

## 2 MODELS AND METHODS

### 2.1 Functional Principal Component Analysis (FPCA)

We model the sample curves as independent realizations of a square integrable stochastic process  $X(t)$  on  $[0, T]$ , with mean  $E\{X(t)\} = \mu(t)$  and covariance function  $\text{cov}\{X(s), X(t)\} = G(s, t)$  (Rice and Silverman, 1991; Capra and Müller, 1997). By Mercer's Theorem,  $G(s, t)$  has an orthogonal expansion in  $L^2([0, T])$ :

$$G(s, t) = \sum_m \lambda_m \rho_m(s) \rho_m(t) \quad m = 1, 2, \dots, \quad (1)$$

where  $\rho_m$  and  $\lambda_m$  are eigenfunctions and eigenvalues ordered by size,  $\lambda_1 \geq \lambda_2 \geq \dots$ .

A random curve from the population then has the following *Karhunen–Loève* representation:

$$X(t) = \mu(t) + \sum_m \varepsilon_m \rho_m(t) \quad 0 \leq t \leq T, \quad (2)$$

where

$$\varepsilon_m = \int_0^T (X(t) - \mu(t)) \rho_m(t) dt \quad (3)$$

are uncorrelated random variables with  $E(\varepsilon_m) = 0$ ,  $E(\varepsilon_m^2) = \lambda_m$ , and  $\sum \lambda_m < \infty$ . The eigenfunctions  $\rho_m$  are referred to as functional principal components (FPCs) with FPC scores  $\varepsilon_m$ .

The deviation of each sample function from the mean is thus represented as a sum of orthogonal curves with uncorrelated random coefficients. We shall suppose that the mean curve and the FPCs are smooth and that the random part can be sufficiently well approximated by the first  $M$  FPCs, for a  $M < \infty$ ; we discuss methods how to choose  $M$  data-adaptively in Supplement (S3).

For a sample of  $n$  random curves observed on a closed interval  $[0, T]$ , let  $X_i = (X_i(t_{i1}), X_i(t_{i2}), \dots, X_i(t_{in_i}))^T$  be the vector of observations for the random curve  $X_i(\cdot)$  at time points  $t_{ij}$ ,  $i = 1, \dots, n$ ,  $j = 1, \dots, n_i$ . An estimate  $\hat{\mu}(t)$  of the mean function  $\mu(t)$  can be obtained by any linear scatterplot smoother (S1).

Forming a dense grid  $s_k$  of  $[0, T]$ , e.g.,  $s_k = \frac{k-1}{S-1}T$ ,  $k = 1, \dots, S$ , for a suitable large  $S$ , the estimation of the covariance function  $G(s, t)$  proceeds via the empirical covariances

$$C_n(s_k, s_l) = \frac{1}{n} \sum_{i=1}^n \{X_i(s_k) - \hat{\mu}(s_k)\} \{X_i(s_l) - \hat{\mu}(s_l)\} \quad (4)$$

for all pairs of times  $(s_k, s_l)$ ,  $k, l = 1, \dots, S$ ,  $k \neq l$ . For the case of irregular time grids, a pre-smoothing step may be included. The empirical covariances are then smoothed, using a two-dimensional scatterplot smoother on the dense grid of points  $(s_k, s_l)$ ,  $k, l = 1, \dots, S$  (S1). A spectral analysis is performed on the resulting  $S \times S$ -matrix  $\hat{G} = (\hat{G}(s_k, s_l))$ , yielding the first  $M$  eigenvectors/eigenvalues for  $\hat{G}$ . The  $m$ th eigenvector is  $(\hat{\rho}_m(s_1), \dots, \hat{\rho}_m(s_S))'$  with the corresponding eigenvalue  $\hat{\lambda}_m$  for  $m = 1, \dots, M$ . The FPC scores  $\hat{\varepsilon}_{im}$  for the  $i$ -th gene and the  $m$ -th FPC are obtained numerically by

$$\hat{\varepsilon}_{im} = \sum_{k=1}^S (X_i(s_k) - \hat{\mu}(s_k)) \hat{\rho}_m(s_k). \quad (5)$$

Alternative shrinkage estimators are described in Yao *et al.* (2003).

Individual temporal gene expression profiles can then be predicted, using their FPC scores, by

$$\hat{X}_i(t) = \hat{\mu}(t) + \sum_{m=1}^M \hat{\varepsilon}_{im} \hat{\rho}_m(t) \quad 0 \leq t \leq T. \quad (6)$$

The FPCA was performed on the combined data set. The FPC scores can then be used to describe both between-group variability and between-group mean differences that may be of relevance for classification. The FPCA methods can be easily extended to cover the case of missing or highly irregular and sparse data (Yao *et al.*, 2005).

## 2.2 Functional Logistic Regression

Generalized linear models are extensions of classical linear models with the following three components (McCullagh and Nelder, 1989): a random component where for the responses,  $Y \sim$  exponential family, with means  $E(Y) = \mu$ ; linear predictors,  $\eta = \sum x_p \beta_p$ , where  $x_p$  is the  $p$ -th predictor variable; and a monotone link function,  $g(\mu) = \eta$ . When  $Y$  is binomial, this is a binomial regression model. A special case is logistic regression where the link function  $g(\cdot)$  is the *logit* function, i.e.,  $\text{logit}(x) = \log\{x/(1-x)\}$ , so that  $g^{-1}(x) = e^x/(1+e^x)$ .

In the framework of the classification problem, the response  $Y$  denotes membership in one of two groups, say  $G_0$  and  $G_1$ , coded as a binary random variable, where  $Y = 1$  if the observation comes from  $G_1$  and  $Y = 0$  if it comes from  $G_0$ . The predictor function  $X(t)$ ,  $t \in [0, T]$  from now on is assumed to be a centered random curve, i.e.,  $\mu(t) \equiv 0$ . For an i.i.d. sample  $X_i(t)$ , for  $i = 1, \dots, n$ , the linear predictors are defined by  $\eta_i = \alpha + \int \beta(t) X_i(t) dt$ , leading to the functional generalized linear model (James, 2002; Müller and Stadtmüller, 2005):

$$Y_i = g^{-1}(\eta_i) + e_i, \quad i = 1, \dots, n, \quad (7)$$

where  $g(\cdot)$  is a link function as before,  $\alpha$  is a constant and  $\beta(\cdot)$  is the parameter function. The errors  $e_i$  are assumed to be independent,  $E(e_i) = 0$ ,  $\text{var}(e_i) < C < \infty$ . The  $M$ -truncated model (see S2) becomes

$$Y_i = g^{-1} \left( \alpha + \sum_{m=1}^M \beta_m \varepsilon_{im} \right) + e_i, \quad i = 1, 2, \dots, n. \quad (8)$$

For fixed  $M$ ,  $\beta^T = (\alpha, \beta_1, \beta_2, \dots, \beta_M)$ , the unknown parameter vector, can be estimated by solving the estimating or score equation

$$U(\beta) = \sum_{i=1}^n (Y_i - \mu_i) g'(\eta_i) \varepsilon_i / \sigma^2(\mu_i). \quad (9)$$

Denote the solution by  $\hat{\beta}^T = (\hat{\alpha}, \hat{\beta}_1, \hat{\beta}_2, \dots, \hat{\beta}_M)$ .

For functional binomial regression, as in classical binomial regression for discriminant analysis, set  $\pi_i = P(Y_i = 1)$  and prior probabilities  $p_1$  and  $p_0$  for the groups  $G_1$  and  $G_0$ , respectively. We estimate  $\pi_i$  by  $\hat{\pi}_i = \hat{P}(Y_i = 1 | X_i(t)) = g^{-1}(\hat{\alpha} + \sum_{m=1}^M \hat{\beta}_m \hat{\varepsilon}_{im})$ . Then we classify the  $i$ -th observation into  $G_1$  if  $\hat{\pi}_i \geq p_1$ , otherwise into  $G_0$ .

## 3 RESULTS

### 3.1 Application to temporal Gene Expression Data for Yeast Cell Cycle

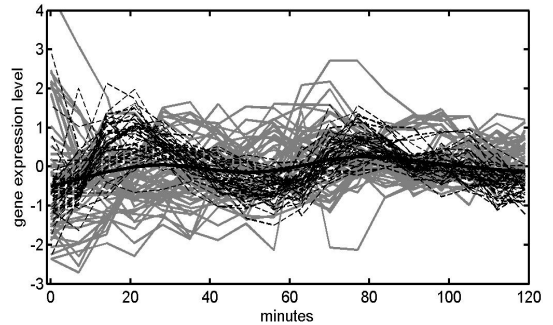
**3.1.1 Functional Discriminant Analysis.** Temporal gene expression data ( $\alpha$  factor synchronized) for the yeast cell cycle were obtained by Spellman *et al.* (1998). There are 6178 genes in total, and each gene expression time-course consists of 18 data points, measured every seven minutes between 0 and 119 minutes. Of 90 genes, which were identified by traditional methods and have data available, 44 are known to be related to G1 phase regulation and 46 to non-G1 phase regulation (i.e. S, S/G2, G2/M and M/G1 phases) of the yeast cell cycle; these serve as the training set. The expression profiles for these 90 genes are depicted in Figure 1, differentiated into phase-specific groups of gene expression profiles in

Figure 2. The estimated covariance surface for these 90 genes in Figure 3 illustrates the pattern of time-dependence of gene expression and provides the basis for constructing the eigenfunctions by spectral decomposition. The diagonal elements  $\hat{C}(s_k, s_l)$  were not used when constructing this surface estimate, as these elements may reflect additional measurement errors.

The number  $M$  of FPCs is chosen by minimizing the leave-one-gene-out cross-validation classification error rate. For each gene in the training set, the FPC scores are estimated from the data of the other 89 genes. Then a functional logistic regression model is fitted for these 89 genes, and group membership for the left-out gene is predicted; this procedure is iterated over all 90 genes, providing the cross-validated predictions.

The solid line in Figure 4 displays the cross-validation classification error rate as a function of  $M$ , the number of FPCs. This plot indicates that when the first five FPCs are used, the overall cross-validation classification error rate is at a minimum 10.00%, with the misclassification rate for G1 genes estimated at 11.36% and for non-G1 genes at 8.70%.

The first five FPCs for the gene expression curves in the training set are depicted in Figure 5. Plotting the FPC scores for the second



**Fig. 1.** Temporal gene expression profiles of yeast cell cycle. Dashed lines: G1 phase; Gray solid lines: non-G1 phases; Black solid line: overall mean curve.

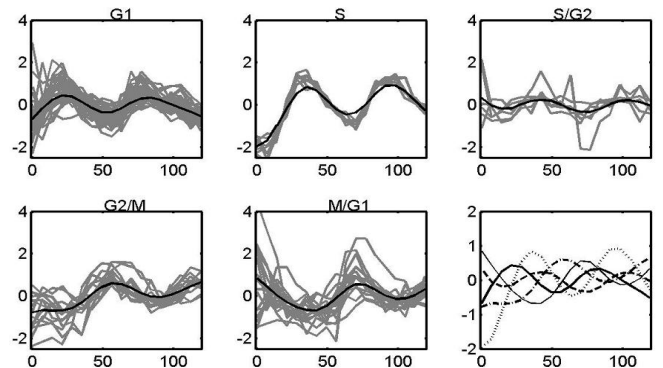


**Fig. 2.** Yeast cell cycle gene expression profiles sorted by phases. The first five panels provide the expression profiles for G1, S, S/G2, G2/M, and M/G1 phases, with mean functions indicated by the black solid lines. The lower right panel contains the mean curves of all phases overlaid: G1 - thick solid line; S - dotted line; S/G2 - dashed line; G2/M - dash-dot line; and M/G1 - thin solid line.

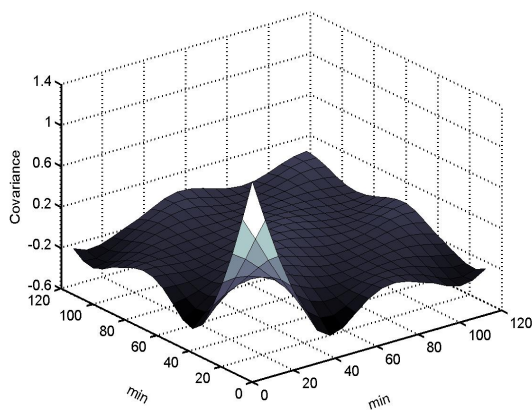


**Fig. 3.** Estimated covariance surface for the 90 known yeast cell cycle genes.

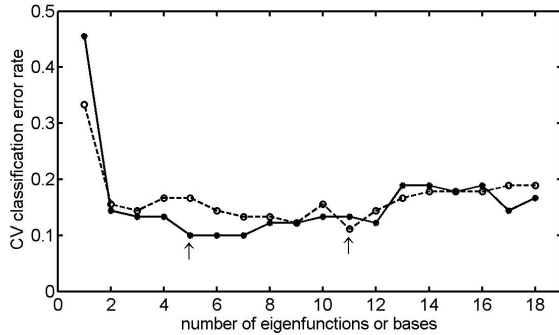


**Fig. 4.** Choosing  $M$ , the number of eigenfunctions for yeast cell cycle data. Leave-one-out cross-validation estimates of the misclassification rate, in dependency on  $M$ : FPCA - solid line; B-spline - dashed line.

FPC versus the first FPC reveals interesting patterns for genes of different phases (Figure 6, left panel). We find that while both G1 and S genes tend to have positive second FPC scores, all the S genes have positive first FPC scores while most G1 genes are on the negative side. On the other hand, most S/G2, G2/M and M/G1 genes have negative second scores; S/G2 and G2/M genes also tend to have positive first FPC scores. The discrimination between S and G1 genes and also between G1/S and non-G1/S genes based on the first two FPC scores is seen to be relatively clear-cut. Similar plots can be produced for each pair of the first five FPC scores. The pairwise scatter plots also highlight the order of the phases. This feature appears to be most evident in the scatter plot of the third versus second FPC scores (Figure 6, right panel). The clockwise order of the genes is G1→S→S/G2→G2/M→M/G1→G1.

A closer look at the misclassified genes showed that there were five genes in the G1 group that were misclassified into the non-G1 group. The left panel of Figure 7 displays four of these five genes, overlaid with the trajectories of G1 genes and S genes. It appears that the trajectories of these genes are in fact close to those of the S genes. The right panel in Figure 7 displays the fifth misclassified gene in the G1 group, overlaid with trajectories of G1 genes and M/G1 genes. This gene's trajectory is seen to be close to the M/G1

trajectories. It appears likely that these five genes are actually non-G1 genes, but somehow were erroneously identified as G1 genes using traditional methods. There are four misclassified genes in the non-G1 group (not shown). Upon close inspection, we find that the trajectories of two of these four genes are closer to those of the G1 group than to those of the non-G1 group. The trajectory of one gene cannot be clearly associated with either group and the fourth gene lies on the boundary of the two groups.

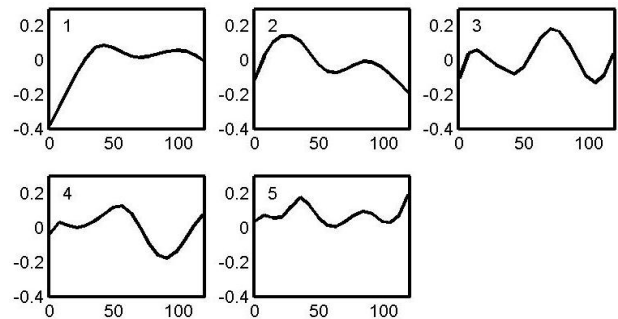


**Fig. 5.** The first five FPCs for the known 90 genes for yeast cell cycle data. These five FPCs account for 98.9% of the total variation, with the first FPC accounting for 66.5%, the second for 21.9%, the third for 4.7%, the fourth for 3.1% and the fifth for 2.7%.

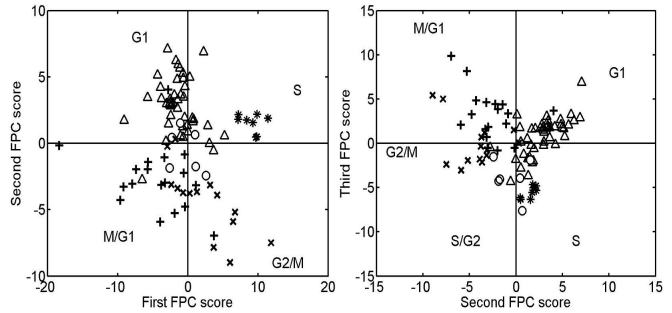


**Fig. 6.** Scatterplot of pairwise FPC scores for genes in the five cell cycle phases. G1 - triangles; S - stars; S/G2 - circles; G2/M - x-marks; M/G1 - plus signs. Left panel: Second versus first FPC score; Right panel: Third versus second FPC scores, for yeast cell cycle data.

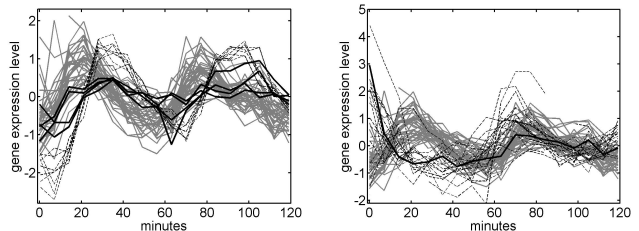


**Fig. 7.** Profiles of misclassified yeast cell cycle genes. Left panel: black solid lines - misclassified G1 genes; gray solid lines - G1 genes; dashed lines - S genes; note that the “misclassified” G1 genes (YDL055C, YDR113C, YDR356W and YJL092W) are actually close to the trajectories of the S genes. Right panel: black solid line - misclassified G1 gene; gray solid lines - G1 genes; dashed lines - M/G1 genes; note that the “misclassified” G1 gene (YCL055W) is actually close to the trajectories of the M/G1 genes. The genes YJL092W and YCL055W were also pointed out by Spellman et al. (1998).

**3.1.2 Comparison with B-Spline Based Method.** Rice and Wu (2001) and Shi *et al.* (1996) proposed a mixed effects model for unequally sampled noisy curves. Let  $X_i = (X_i(t_{i1}), X_i(t_{i2}), \dots, X_i(t_{in_i}))^T$  be the vector of observations for the  $i$ th curve for  $i = 1, 2, \dots, n$ , where  $X_{ij} = X_i(t_{ij})$  is the observed function value at time  $t_{ij}$ ,  $j = 1, \dots, n_i$ . Note that the setup is the same as described above.

The approximating model of Rice and Wu is:

$$X_{ij} = \sum_{k=1}^p \beta_k \bar{B}_k(t_{ij}) + \sum_{l=1}^q \gamma_{il} B_l(t_{ij}) + \varepsilon_{ij},$$

where the mean function is  $E(Y_i(t)) = \mu(t) = \sum_{k=1}^p \beta_k \bar{B}_k(t)$ , and  $\bar{B}_k(\cdot)$ ,  $B_l(\cdot)$  are possibly different B-spline bases on  $[0, T]$ . The  $\gamma_{il}$  are random effects, with  $E(\gamma_{il}) = 0$  and  $\text{cov}(\gamma_{il}) = \Gamma$ . The corresponding estimate of an individual trajectory is the smooth curve

$$\hat{X}_i(t) = \sum_{k=1}^p \hat{\beta}_k \bar{B}_k(t) + \sum_{l=1}^q \hat{\gamma}_{il} B_l(t),$$

where the estimates are obtained by least squares. Classification can be based on the random coefficients  $\gamma_{il}$ , and the dashed line in Figure 4 shows the overall misclassification error rates. Using B-splines, the misclassification error rate attains its lowest value 11.1% when using eleven bases, while the minimum error rate using FPCA is 10% and is achieved with only five FPCs, as described above. Thus FPCA is seen to be advantageous in this example by employing fewer components than the B-Spline approach, while simultaneously yielding a slightly lower misclassification error rate.

### 3.2 Application to Expression Patterns of Cell-type specific Genes in *Dictyostelium*

Iranfar et al. (2001) studied expression patterns of cell-type specific gene fragments in *Dictyostelium discoideum*. Such studies are of particular interest for *Dictyostelium*, since only prestalk and prespore cells are differentiated during development. DNA microarrays carrying 690 targets were used to determine expression profiles during development. Fitting a biologically based kinetic equation to extract the times of transcription onset and cessation, the authors recognized 35 cell-type specific genes, including 17 newly identified ones, which were confirmed by Northern blots. We used these 35 genes, with 14 prestalk genes and 21 prespore genes, as our training set to explore other potential cell-type specific genes. Figure 8 shows the relative intensity of the signals for prestalk and prespore genes. A considerable number of prestalk genes peaked between 8 and 10 hours of development and then decreased significantly, while most prespore genes were not expressed until 10 hours of development and continued to be expressed thereafter.

We used these genes as training set for functional discriminant analysis. Cross-validation error rates indicated that using the first three FPCs yields the lowest overall misclassification rate of 22.86%, with 28.57% for prestalk genes and 19.05% for prespore genes. Misclassified prestalk genes are highlighted in the left panel of Figure 9. Besides *emcA* and *emcB*, which were screened out by Iranfar et al. (2001) due to their “prespore-like” profiles, we found that *ostB* and *mitA* might not be correctly classified either. These two genes show no cell-type specific features yet were grouped into prestalk genes. For another gene *rasD*, mentioned by Iranfar (2001), the estimated probability for classification into prespore genes with

0.4376 only slightly exceeds the threshold of 0.4, which is the prior probability according to the training set. The right panel of Figure 9 highlights the four misclassified prespore-specific genes. Gene *cbpB* shows an early peak at 8 hours, and follows the pattern of prestalk genes. Genes *sodA* and *thfA* did not show obvious cell-specific features in their expression patterns. Gene *cprF* did not start to express until 20 hours, which may have contributed to its misclassification.

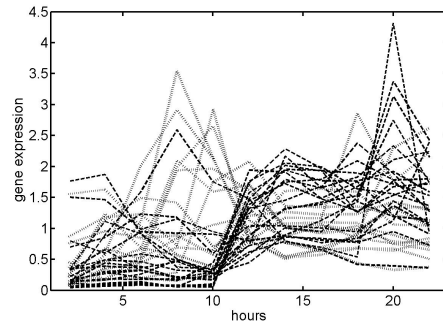


**Fig. 8.** Developmental temporal patterns of *Dictyostelium* gene expression. Dotted lines - prestalk-specific genes; dashed lines - prespore-specific genes.

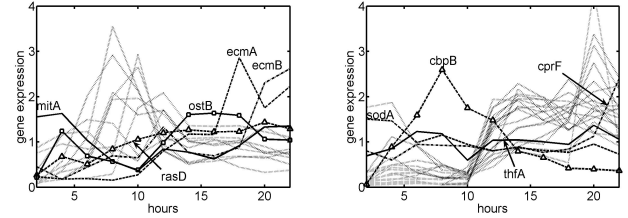


**Fig. 9.** Misclassified cell-type specific genes for *Dictyostelium*. Left panel: Prestalk genes are shown in light gray. The four misclassified prestalk-specific genes are labelled and highlighted in thick lines; gene *rasD* is also indicated (see text). Right panel: Prespore genes are shown in light gray. The four misclassified prespore-specific genes are labelled and highlighted in thick lines.

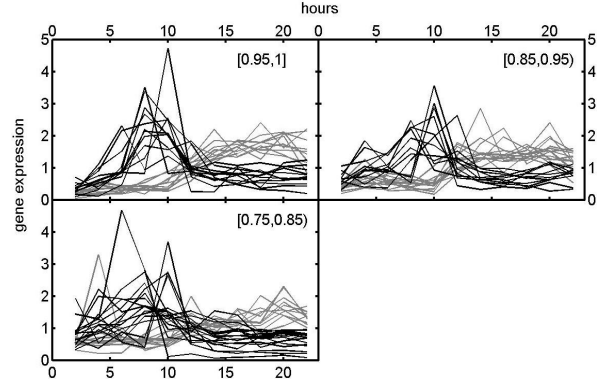


**Fig. 10.** Subgroups of *Dictyostelium* cell-type specific genes according to different posterior probabilities. Black solid lines - Prestalk-specific genes corresponding to the indicated range of posterior probabilities; gray solid lines - Prespore-specific genes corresponding to posterior probabilities of  $[0, 0.05]$  (upper left panel),  $(0.05, 0.15]$  (upper right panel) and  $(0.15, 0.25]$  (lower panel).

We then used the model fitted to the training set to classify the rest of the genes, and chose ranges of estimated probabilities for a gene to be classified into the prestalk group of  $[0.95, 1]$ ,  $[0.85, 0.95]$  and  $[0.75, 0.85]$ , in order to identify subgroups of prestalk genes. Analogous probability ranges of  $[0, 0.05]$ ,  $(0.05, 0.15]$  and  $(0.15, 0.25]$  were used to identify subgroups of prespore genes. The results are shown in Figure 10. With these three classification probability ranges, 40 prestalk-specific and 36 prespore-specific genes were identified, displaying reasonably homogeneous patterns within each identified subgroup. Especially the genes in the left upper panel show very typical cell-specific patterns.

### 3.3 A Simulation Study

**3.3.1 Functional Discriminant Analysis.** A data-based simulation study was performed based on the first five estimated FPCs from the yeast cell cycle data, where we assume that these correspond to the real underlying FPCs. Then five random coefficients  $\varepsilon_m, m = 1, \dots, 5$ , were generated for each subject from normal distributions with means 0.6, 0.5, 0.4, 0.3, and 0.2 for group 1 and  $-0.6, -0.5, -0.4, -0.3$ , and  $-0.2$  for group 2, with variances  $\sigma_m^2 = 2.6950, 0.8850, 0.1957, 0.1266$  and 0.1079 for both groups. These variances correspond to the estimated eigenvalues from the yeast cell cycle data. The priors for the two groups were chosen equal, i.e.  $\pi_1 = \pi_2 = \frac{1}{2}$ , so that the generated samples have overall mean 0. For all subjects, 18 equally spaced data points were taken, just as is the case for the yeast cell cycle data. We generated 100 training and test data sets. Each data set was composed of 200 samples, where the first 100 samples formed the training set and the remaining 100 samples the test set.

For each of the 100 simulated data sets, classification error rates were calculated for the test data based on FPCA and B-spline methods, respectively. The simulation classification error rates based on FPCA and B-splines are compared in Table 1 (Monte Carlo standard errors are in parentheses). The average classification error rate over the 100 data sets indicates that all five FPCs should be used for optimal classification with either method. Except for the case with one eigenfunction/base function, the overall classification error rates based on FPCA are always slightly lower than those observed for B-splines.

## 4 DISCUSSION AND CONCLUSIONS

Because of the dynamic nature of biological systems, temporal gene expression data play a critical role in exploring the regulation of gene expression, in particular, in highlighting genes that are time critical for the regulation of certain biological processes such as the cell cycle for different organisms (Spellman *et al.* 1998; Laub *et al.*, 2000; Breyne *et al.*, 2001; and Cho *et al.*, 2001), the central nervous system development (Wen *et al.*, 1998), *Drosophila* development (White *et al.*, 1999; Arbeitman *et al.*, 2002) and

**Table 1.** Classification Error Rates Based on FPCA and B-Splines (B-S).

no. of FPC or base function	Group 1		Group 2		overall	
	FPCA	B-S	FPCA	B-S	FPCA	B-S
1	32.7(0.07)*	30.5(0.07)	33.0(0.08)	29.8(0.07)	32.8(0.05)	30.1(0.04)
2	27.8(0.07)	36.8(0.09)	26.1(0.07)	37.5(0.08)	27.0(0.04)	37.2(0.05)
3	11.4(0.05)	14.6(0.05)	11.9(0.05)	15.0(0.05)	11.7(0.03)	14.8(0.03)
4	10.8(0.05)	11.2(0.05)	10.3(0.05)	11.2(0.05)	10.6(0.03)	11.2(0.03)
5	10.3(0.04)	10.8(0.05)	10.3(0.05)	10.7(0.05)	10.3(0.03)	10.8(0.03)

*Dictyostelium* cell differentiation (Iranfar *et al.*, 2001). With rapidly accumulating amounts of temporal microarray gene expression data, developing adequate models to analyze such data is urgent. In this paper, we propose a functional discriminant analysis method, using a functional version of logistic regression and functional principal components for the temporal gene expression data.

Temporal gene expression data provide valuable functional information about temporal patterns of gene expression and also interactions between genes. For example, a typical yeast mitotic cell cycle is commonly broken down into the four standard phases: G1, S, G2, and M. When the daughter cell breaks away from the mother cell, it is typically smaller than the mother cell. During the G1 phase, the daughter cell will grow until it is of a large enough size to enter the cell cycle. The G1 phase of the cell cycle is important for determining the fate of the cell. Statistically identifying genes that regulate the G1 phase will be helpful for studies of genetic cell cycle regulation. Since most biological processes are in fact continuous, temporal gene expression data can be viewed as discretized samples from smooth random gene expression trajectories over time, naturally leading to a functional data analysis approach. The proposed method provides low error rate (10%) classification for the yeast cell cycle gene expression data and also in simulations. Differentiating cell cycle regulated genes from non-cell-cycle-regulated genes is another important goal for cell cycle studies. Extensions of the functional methods proposed here will be of interest in approaching this problem.

In comparisons with the B-spline approach, both yeast cell cycle data analysis and simulations demonstrate overall lower error rates with fewer eigenfunctions/base functions when using the FPCA method. The proposed FPCA methods allow the identification of genes that were likely misclassified by traditional biological classification methods. The phase order displayed by scatterplots of pairwise FPC scores suggests that FPCA has potential for time ordination analysis of temporal gene expression.

The NIH has designated *Dictyostelium discoideum* as a model organism for the functional analysis of sequenced genes. Applying our methods, we screened out previously misclassified cell-type specific genes. Furthermore, we identified 76 genes falling into subgroups that show cell-type specific features of gene expression. Extending the proposed algorithm to functional cluster analysis is feasible and useful in the common situation where group membership is unknown, as is often the case in biological applications.

## ACKNOWLEDGEMENTS

The comments of three reviewers led to numerous improvements and are gratefully acknowledged. Research supported in part by NSF grants DMS03-54448 and DMS05-05537.

## REFERENCES

- Aach, J. and Church, G.M. (2001) Alignment gene expression time series with time warping algorithms. *Bioinformatics*, **17**, 495-508.
- Alter, O., Brown, P.O. and Botstein, D. (2000) Singular value decomposition for genome-wide expression data processing and modelling. *Proc. Natl Acad. Sci. U.S.A.*, **97**, 10101-10106.
- Alter, O., Brown, P.O. and Botstein, D. (2003) Generalized singular value decomposition for comparative analysis of genome-scale expression data sets of two different organisms. *Proc. Natl Acad. Sci. U.S.A.*, **100**, 3351-3356.
- Arbeitman, M.N., Furlong, E.E.M., Imam, F., Johnson, E., Null, B.H., Baker, B.S., Krasnow, M.A., Scott, M.P., Davis, R.W. and White, K.P. (2002) Gene expression during the life cycle of *Drosophila melanogaster*. *Science*, **297**, 2270-2275.

- Bar-Joseph, Z., Gerber, G., Gifford, D.K., Jaakkola, T.S. and Simon I. (2003) Continuous representation of time-series gene expression data. *Journal of Computational Biology*, **10**, 341-356.
- Breyne, P. and Zabeau, M. (2001) Genome-wide expression analysis of plant cell cycle modulated genes. *Current Opinion in Plant Biology*, **4**, 136-142.
- Brown, M.P.S., Grundy, W.N., Lin, D., Cristianini, N., Sugnet, C.W., Furey, T.S., Ares, M. and Haussler, D. (2000) Knowledge-based analysis of microarray gene expression data by using support vector machines. *Proc. Natl Acad. Sci. U.S.A.*, **97**, 262-267.
- Capra, W.B. and Müller, H.G. (1997) An accelerated-time model for response curves. *J. Am. Statist. Ass.*, **92**, 72-83.
- Cho, R.J., Campbell, M.J., Winzeler, E.A., Steinmetz, L., Conway, A., Wodicka, L., Wolfsberg, T.G., Gabrielian, A.E., Landsman, D., Lockhart, D.J. and Davis, R.W. (1998) A genome-wide transcriptional analysis of the mitotic cell cycle. *Mol. Cell*, **2**, 65-73.
- Cho, R.J., Huang, M., Campbell, M.J., Dong, H., Steinmetz, L., Sapinoso, L., Hampton, G., Elledge, S.J., Davis, R.W. and Lockhart, D.J. (2001) Transcriptional regulation and function during the human cell cycle. *Nature Genet.*, **27**, 48-54.
- Efron, B. (1975) The efficiency of logistic regression compared to normal discriminant analysis. *J. Am. Statist. Ass.*, **70**, 892-898.
- Eisen, M.B., Spellman, P.T., Brown, P.O. and Botstein, D. (1998) Cluster analysis and display of genome-wide expression patterns. *Proc. Natl Acad. Sci. U.S.A.*, **95**, 14863-14868.
- Fan, J. and Gijbels, I. (1996). *Local Polynomial Modelling and its Applications*. Chapman & Hall, New York.
- Gasch, A.P., Spellman, P.T., Kao, C.M., Carmel-Harel, O., Eisen, M.B., Botstein, D. and Brown, P.O. (2000) Genomic expression programs in the response of yeast cells to environmental changes. *Mol. Bio. Cell*, **11**, 4241-4257.
- Golub, T.R., Slonim, D.K., Tamayo, P., Huard, C., Gaasenbeek, M., Mesirov, J.P., Coller, H., Loh, M.L., Downing, J.R., Caligiuri, M.A., Bloomfield, C.D. and Lander, E.S. (1999) Molecular classification of cancer: class discovery and class prediction by gene expression monitoring. *Science*, **286**, 531-537.
- Hall, P., Poskitt, D.S. and Presnell, B. (2001) A functional data-analytic approach to signal discrimination. *Technometrics*, **43**, 1-9.
- Hill, A.A., Hunter C.P., Tsung B.T., Tucker-Kellogg, G. and Brown, E.L. (2000) Genomic analysis of gene expression in *C. elegans*. *Science*, **290**, 809-812.
- Holter, N.S., Mitra, M., Maritan, A., Cieplak, M., Banavar, J. and Fedoroff, N.V. (2000) Fundamental patterns underlying gene expression profiles: simplicity from complexity. *Proc. Natl Acad. Sci. U.S.A.*, **97**, 8409-8414.
- Iranfar, N., Fuller, D., Sasik, R., Hwa, T., Laub, M. and Loomis, W.F. (2001) Expression patterns of cell-type specific genes in *Dictyostelium*. *Mol. Bio. Cell*, **12**, 2590-2600.
- Iyer, V.R., Eisen, M.B., Ross, D.T., Schuler, G., Moore, T., Lee, J.C.F., Trent, J.M., Staudt, L.M., Jr. Hudson, J., Boguski, M.S., Lashkari, D.L., Shalon, D., Botstein, D. and Brown, P.O. (1999) The transcriptional program in the response of human fibroblasts to serum. *Science*, **283**, 83-87.
- James, G.M. and Hastie, T.J. (2001) Functional linear discriminant analysis for irregular sampled curves. *J. R. Statist. Soc. B*, **63**, 533-550.
- James, G.M. (2002) Generalized linear models with functional predictors. *J. R. Statist. Soc. B*, **64**, 411-432.
- Klevecz, R.R. and Murray, D.B. (2001) Genome wide oscillations in expression: wavelet analysis of time series data from yeast expression arrays uncovers the dynamic architecture of phenotype. *Molecular Biology Reports*, **28**, 73-82.
- Kruglyak, S. and Tang, H. (2001) A new estimator of significance of correlation in time series data. *Journal of Computational Biology*, **8**, 463-470.
- Laub, M.T., McAdams, H.H., Feldblyum, T., Fraser, C.G. and Shapiro, L. (2000) Global analysis of the genetic network controlling a bacterial cell cycle. *Science*, **290**, 2144-2148.
- Lee, S.I. and Batzoglou, S. (2003) Application of independent component analysis to microarrays. *Genome Biology*, **4**, Art. R76.
- Li, K.C., Yan, M. and Yuan, S. (2002) A simple statistical model for depicting the cdc15-synchronized yeast cell-cycle regulated gene expression data. *Statistica Sinica*, **12**, 141-158.
- Liebermeister, W. (2002) Linear modes of gene expression determined by independent component analysis. *Bioinformatics*, **18**, 51-60.
- Liu, X.L. and Müller, H.G. (2003) Modes and clustering for time-warped gene expression profile data. *Bioinformatics*, **19**, 1937-1944.
- Luan, Y.H. and Li, H.Z. (2003) Clustering of temporal gene expression data using a mixed-effects model with B-splines. *Bioinformatics*, **19**, 474-482.
- Lukashin, A.V. and Fuchs, R. (2001) Analysis of temporal gene expression profiles: clustering by simulated annealing and determining the optimal number of clusters. *Bioinformatics*, **17**, 405-414.
- McCullagh, P. and Nelder, J.A. (1989) *Generalized Linear Models*. Chapman & Hall, London.
- Mohanty, S. and Firtel, R.A. (1999) Control of spatial patterning and cell-type proportioning in *Dictyostelium*. *Semin. Cell Dev. Biol.*, **10**, 597-607.
- Müller, H.G. (2005) Functional modelling and classification of longitudinal data. *Scandinavian J. Statistics*, **32**, 223-240.
- Müller, H.G. and Stadtmüller, U. (2005) Generalized functional linear models. *Annals of Statistics*, **33**, 774-805.
- Nikkila, J., Toronen, P., Kaski, S., Venna, J., Castren, E. and Wong, G. (2002) Analysis and visualization of gene expression data using self-organizing maps. *Neural Networks*, **15**, 953-966.
- Press, S.J. and Wilson, S. (1978) Choosing between logistic regression and discriminant analysis. *J. Am. Statist. Ass.*, **73**, 699-705.
- Peng, X., Karuturi, R.K.M., Miller, L.D., Lin, K., Jia, Y., Kondu, P., Wang, L., Wong, L.S., Liu, E.T., Balasubramanian, M.K. and Liu, J. (2005) Identification of Cell Cycle-regulated Genes in Fission Yeast. *Mol. Biol. Cell*, **16**, 1026-1042.
- Qin, J., Lewis, D.P. and Noble, W.S. (2003) Kernel hierarchical gene clustering from microarray expression data. *Bioinformatics*, **19**, 2097-2104.
- Ramsay, J.O. and Silverman, B.W. (2005) *Functional Data Analysis*. Springer, New York.
- Raychaudhuri, S., Stuart, J.M. and Altman, R.B. (2000) Principal components analysis to summarize microarray experiments: application to sporulation time series. *Pacific Symposium on Biocomputing*, Winter, 455-466.
- Resson, H., Wang, D.L. and Natarajan, P. (2003) Clustering gene expression data using adaptive double self-organizing map. *Physiological Genomics*, **14**, 35-46.
- Rice, J.A. and Silverman, B.W. (1991) Estimating the mean and covariance structure nonparametrically when the data are curves. *J. R. Statist. Soc. B*, **53**, 233-243.
- Rice, J.A. and Wu, C.O. (2001) Nonparametric mixed effects models for unequally sampled noisy curves. *Biometrics*, **57**, 253-259.
- Rustici G., Mata J., Kivinen K., Lio P., Penkett C.J., Burns G., Hayles J., Brazma A., Nurse P. and Bahler J. (2004) Periodic gene expression program of the fission yeast cell cycle. *Nature Genetics*, **36**, 809-817.
- Schena, M., Shalon, D., Davis, R.W. and Brown, P.O. (1995) Quantitative monitoring of gene expression patterns with a complementary DNA microarray. *Science*, **270**, 467-470.
- Schena, M., Shalon, D., Heller, R., Chai, A., Brown, P.O. and Davis, R.W. (1996) Parallel human genome analysis: microarray-based expression monitoring of 1000 genes. *Proc. Natl Acad. Sci. U.S.A.*, **93**, 10614-10619.
- Shaulsky, G. and Loomis, W.F. (2002) Gene expression patterns in *Dictyostelium* using microarrays. *Protist*, **153**, 93-8.
- Shi, M.G., Weiss, R.E. and Taylor, J.M.G. (1996) An analysis of paediatric CD4 counts for acquired immune deficiency syndrome using flexible random curves. *J. R. Statist. Soc. C*, **45**, 151-163.
- Spellman, P.T., Sherlock, G., Zhang, M.Q., Iyer, V.R., Anders, K., Eisen, M.B., Brown, P.O., Botstein, D. and Futcher, B. (1998) Comprehensive identification of cell cycle-regulated gene of the yeast *Saccharomyces cerevisiae* by microarray hybridization. *Mol. Biol. Cell*, **9**, 3273-3297.
- Tavazoie, S., Hughes, J.D., Campbell, M.J., Cho, R.J. and Church, G.M. (1999) Systematic determination of genetic network architecture. *Nature Genet.*, **22**, 281-285.
- Tamayo, P., Slonim, D., Mesirov, J., Zhu, Q., Kitareewan, S., Dmitrovsky, E., Lander, E.S. and Golub, T.R. (1999) Interpreting pattern of gene expression with self-organizing maps: methods and application to hematopoietic differentiation. *Proc. Natl Acad. Sci. U.S.A.*, **96**, 2907-2912.
- Wen, X., Fuhrman, S., Michaels, G.S., Carr, D.B., Smith, S., Barker, J.L. and Somogyi, R. (1998) Large-scale temporal gene expression mapping of central nervous system development. *Proc. Natl Acad. Sci. U.S.A.*, **95**, 334-339.
- White K.P., Rifkin, S.A., Hurban, P. and Hogness, D.S. (1999) Microarray analysis of *Drosophila* development during metamorphosis. *Science*, **286**, 2179-2184.
- Wu, F.X., Zhang, W.J. and Kusalik, A.J. (2003) A genetic K-means clustering algorithm applied to gene expression data. *Lecture in Artificial Intelligence*, **2671**, 520-526.
- Yao, F., Müller, H.G. and Wang, J.L. (2005) Functional Data Analysis for Sparse Longitudinal Data. *J. Am. Statist. Ass.*, **100**, 577-590.
- Yao, F., Müller, H.G., Clifford, A.J., Dueker, S.R., Follett, J., Lin, Y.M., Buchholz, B.A. and Vogel, J.S. (2003) Shrinkage estimation for functional principal component scores with application to the population kinetics of plasma folate. *Biometrics*, **59**, 676-685.
- Zhao, X., Marron, J.S. and Wells, M.T. (2004) The functional data analysis view of longitudinal data. *Statistica Sinica*, **14**, 789-808.